94-020



*Zbigniew Lewandowski,*[1] *Thomas Funk,*[1] *Frank Roe,*[1] *and Brenda J. Little*[2]

# Spatial Distribution of pH at Mild Steel Surfaces Using an Iridium Oxide Microelectrode

**REFERENCE:** Lewandowski, Z., Funk, T., Roe, F., and Little, B., **"Spatial Distribution of pH at Mild Steel Surfaces Using an Iridium Oxide Microelectrode,"** *Microbiologically Influenced Corrosion Testing, ASTM STP 1232,* Jeffery R. Kearns and Brenda J. Little, Eds., American Society for Testing and Materials, Philadelphia, 1994, pp. 61–69.

**ABSTRACT:** The distribution of pH near a metal surface indicates the positions of anodic (low pH) and cathodic sites (high pH). A microsensor, small enough that the pH sensing tip is confined to the diffusion layer, can be used to monitor pH near metal surfaces. This paper describes the mapping of pH near water-immersed mild steel surfaces using miniaturized iridium/iridium oxide pH microelectrodes in conjunction with a computer controlled micropositioner and data acquisition system. Two systems were analyzed: (1) a bare mild steel coupon exposed to artificial sea water, and (2) a mild steel coupon, first partially covered with the biopolymer, calcium alginate, and then exposed to artificial seawater. After 8 h exposure to seawater both coupons exhibited localized corrosion. On the coupon partially covered with calcium alginate gel, corrosion was limited to the area covered by biopolymer. On the bare coupon, corrosion was widespread. pH mapping of the coupons showed that low pH regions were identified with the corroded areas, and high pH regions with the uncorroded areas. These observations demonstrate that, in the abiotic environment, anodic sites on a mild steel surface can be fixed by partially covering the metal with biopolymer.

**KEYWORDS:** microelectrode, pH, iridium oxide, mapping, corrosion, mild steel, alginate, biopolymer, microbiologically influenced corrosion (MIC)

Microorganisms growing on water immersed metal surfaces form biofilms that are held together by extracellular polymeric substances (EPS). This type of microbial colonization is frequently associated with microbially influenced corrosion (MIC). The mechanisms relating microbial colonization and corrosion are not well understood. MIC costs the U.S. economy billions of dollars each year.

MIC is a function of a variety of environmental factors such as: metal alloy composition (for example, mild steel versus stainless steel), biofilm properties (for example, aerobic versus anaerobic organisms), and fluid characteristics (temperature, hydrodynamics, chemical composition) [*1,2*]. Corrosion mechanisms can be analyzed in terms of the anodic and cathodic processes that are occurring [*3*].

The rate limiting step of corrosion can be either oxidation of the metal or reduction of oxygen. Bare mild steel corrodes in dilute saline solutions showing no pronounced polari-

[1] Associate professor of civil engineering, and research associates, respectively, Montana State University, Bozeman, MT.
[2] Research chemist, Naval Oceanographic and Atmospheric Research Station, Stennis Space Center, MS.

zation; passivation rarely takes place and corrosion rates normally increase as corrosion potentials increase [4]. In this case, reduction of oxygen is normally the rate-limiting step due to diffusional or mixed diffusion/reaction control [5].

Biofilms have been implicated in both inhibition and promotion of corrosion of mild steel. Hernandez-Duque et al. [6] reported a drop in the corrosion rate of mild steel in the presence of a uniform layer of biofilm. This drop was attributed to respiration of the biofilm that resulted in a decline in oxygen concentration at the metal surface and associated decrease in rate of cathodic reduction oxygen. Smith et al. [7] reported the agar coated steel (artificial biofilm) also produced a very high polarization resistance and low corrosion rate. The last result suggests that biofilm metabolic activity may not be necessary for inhibition of corrosion by biopolymers.

Many researchers, on the other hand, have reported that biofilms promote MIC on mild steel surfaces [8]. Iverson [9] proposed that the natural patchiness of biofilms results in differential aeration cells at the metal surface; areas with more biofilm exhibit low oxygen concentrations and become anodic, while those with less biofilm are exposed to higher oxygen concentrations and become cathodic. This patchiness can also cause concentration gradients of other electrochemically active species within the biofilm [10]. Heterogeneities in biofilm structure and composition may be the key factor in determining whether biofilms enhance or inhibit corrosion rates. Consequently, MIC may not depend entirely on metabolically active biofilms.

This paper describes localized corrosion of mild steel in aerobic seawater. The role of biofilms in this process is under investigation. From the cited literature it is not clear if patchiness of biofilms alone promotes MIC to the extent observed, or whether some metabolic activity is necessary. Our study addresses the hypothesis that metabolic activity of biofilms is not always necessary in promoting MIC. This hypothesis was verified by forming an artificial patchy biofilm by partially coating a bare mild steel surface with the biopolymer, calcium alginate, and observing the location and extent of corrosion. If a differential aeration cell formed, localized corrosion would occur under the alginate and oxygen reduction would occur on the adjacent bare surface. A map of pH in the vicinity of the alginate spot should show a decrease in pH above the anodic site (the alginate spot) and an increase in pH above the cathodic site (bare surface).

## Experimental Approach

### *Overview*

A polished mild steel coupon was partially covered with calcium alginate biopolymer gel and immersed in artificial seawater. An iridium/iridium oxide pH microelectrode was used to map pH above the immersed coupon; results were compared to similar measurements over a bare polished control coupon.

### *Electrode Construction and Calibration*

Briefly, an iridium wire is tapered electrochemically and covered with glass (Fig. 1). Excess glass is ground off to expose the tip of the iridium wire. The wire is then recessed a few micrometers into the glass to provide a protected area for the active iridium oxide. The iridium oxide layer is formed by potential cycling. This technique alternatively applies oxidation and reduction potentials to the exposed metal tip, oxidation being the slightly dominant process. The electrode tip is finally cleaned, aged in water, and calibrated. Details for electrode construction are given in the paper by VanHoudt et al. [11].

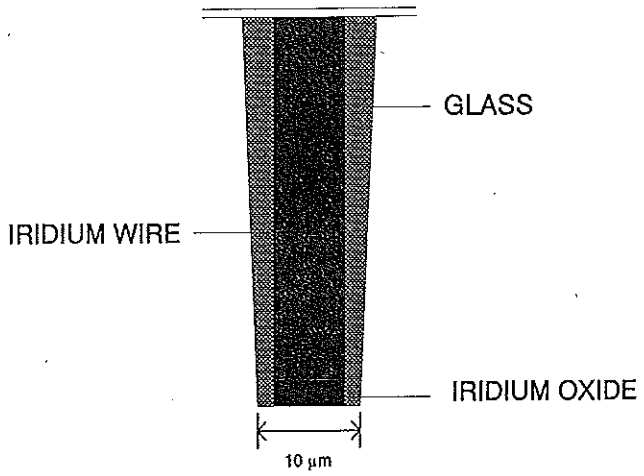


FIG. 1—*Tip of an iridium oxide pH microelectrode.*

*Aging the Electrode*—The pH-sensitive oxide is composed of hydrous and anhydrous iridium oxides. The degree of hydration changes with time causing a drift in calibration [*12*]. Furthermore, there is little consistency in the measured slope (mV/pH) for electrodes prepared using a single process. For electrochemically prepared electrodes, Kinoshita et al. [*13*] report 69.7 mV/pH-unit and Hitchman and Ramanathan [*14*] report 81.9 mV/pH-unit at 25°C. Our measurements indicated an initial slope of 77.3 mV/pH-unit that decreased after one week to 65.8 mV/pH-unit. Because the greatest change in oxide hydration occurs during the first 12 hours of equilibration [*12*], electrodes were aged in distilled water for 12 hours followed by aging in air for 2 hours. Data collected four times during the course of one week are shown in Fig. 2. Electrodes were stored in air.

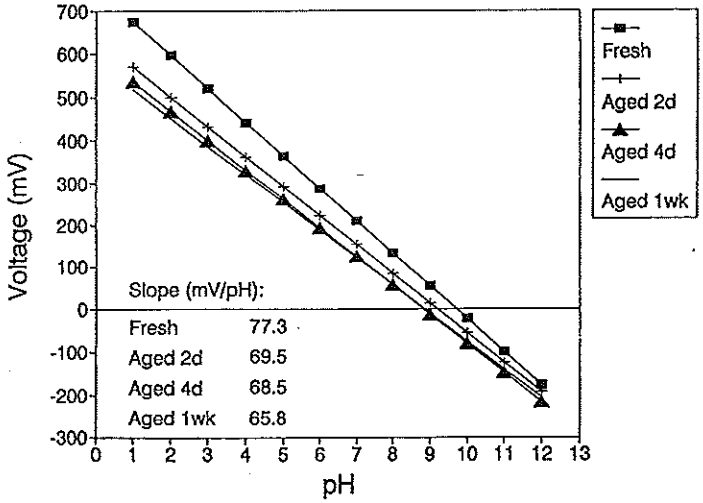


FIG. 2—*The effect of aging on pH response of an iridium/iridium oxide microelectrode.*

*Calibration*—Experimentation has shown that the internal impedance of iridium/iridium oxide microelectrodes can be as much as $10^{10}$ Ω. An electrometer with a minimum input impedance of $10^{12}$ Ω is used to measure the microelectrode potential relative to a reference electrode. This high impedance ensures that the meter does not load the electrode. A meter with an input impedance comparable to, or less than, $10^{10}$ Ω would produce inaccurate results by acting as a voltage divider. A low impedance volt meter can also damage the sensor by allowing current to flow through it. As a final caveat, the sensor should never be short-circuited to the reference electrode while both are in solution, since the voltage difference would cause current to flow and damage the electrode.

A World Precision Instruments model FD 223 electrometer (impedance = $10^{15}$ Ω) was used to measure pH from 1 to 12. The reference was Ag/AgCl with an internal fill solution of $Ag^+$ saturated 3M KCl. The Nernstian slope was 77.3 mV/pH-unit and E° was 751 mV. Slopes of 70 to 80 mV/pH unit were typical of freshly prepared electrodes. As noted above, slopes usually settled to ≈65 mV/pH-unit after several calibrations and uses, or both, as reported above. Response was immediate for most pH buffers.

Although Midgley [*15*] reported that the iridium/iridium oxide pH electrode was not sensitive to $Fe^{2+}$ and $Fe^{3+}$ ions, we found that the presence of $Fe^{2+}$ did influence the response of the electrode. Increasing the ferrous ion concentration led to underestimating the acidic nature of the media by, at most, one pH unit. Valid qualitative conclusions can be drawn in spite of this interference.

### *Surface Mapping pH Near the Metal Surface*

An iridium/iridium oxide pH microelectrode was used to map pH over metal coupon surfaces. The coupons were mounted in the bottom of a rectangular polycarbonate vessel located on an XY-axis positioning table. The pH microelectrode was mounted on the shaft of a stationary Z-axis positioner above the coupon. The polycarbonate vessel was filled with artificial sea water (Instant Ocean® Aquarium Systems, Mentor, OH), and guided under computer control in a plane perpendicular to the stationary pH probe. Measurements taken at 100 μm intervals in two dimensions were used to construct an evenly spaced grid of pH data. The experimental apparatus is shown schematically in Fig. 3. All corrosion and surface mapping took place at room temperature.

*XYZ micropositioner*—The micropositioning system was manufactured by Micro Kinetics (Laguna Hills, CA). The XY table consisted of an X-Y stage with 4 in. travel driven by two encoder motors with gear heads. The Z-positioner consisted of a Drivemaster™ (Microkinetics) positioner with a gear ratio of 1670:1 and a maximum travel of 1 in. The XYZ-positioning system had a resolution of 0.1 μm. A three axis motor controller, connected to a personal computer through an RS232 serial interface, provided control of the positioning motors. Custom software integrated the motion of the positioner with collection of data. The large matrix of pH versus X and Y coordinates was plotted in three dimensions using Graph Tools™ (3D Vision Corp. Torrance, CA) software.

*Polycarbonate reaction vessel*—Mild steel coupons (diameter = 1.6 cm) were embedded in threaded PVC plugs using epoxy cement. A reaction vessel was made of 1.27-cm-thick polycarbonate. The vessel was 5-cm square and 2-cm deep with a raised bottom into which the coupons were mounted (Fig. 3).

*Coupon preparation*—The coupons, which had been previously mounted in PVC plugs, were cleaned and brought to near-mirror smoothness by polishing with graded silicon carbide sand papers down to a 1200 grit coarseness. They were then rinsed with distilled water and air dried.

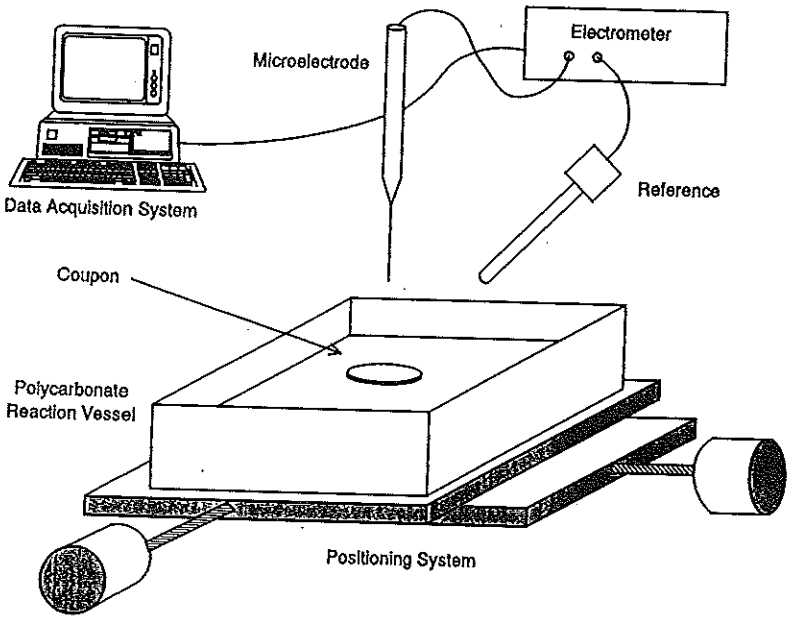


FIG. 3—*Experimental apparatus.*

*Control coupon*—Localized corrosion was induced on a clean bare mild steel coupon surface by masking all but a portion of it (0.04 $cm^2$) with water proof tape and immersing it in artificial seawater (Instant Ocean) for approximately 8 h at room temperature. This procedure created intense localized corrosion in the exposed region. The tape was removed just before scanning.

*Corrosion of a coupon coated with a spot of calcium alginate gel*—Another clean, bare, mild, steel coupon was also masked with waterproof vinyl tape except for a 0.04 $cm^2$ area in the middle of the coupon. The exposed area was sprayed with 0.4% sodium alginate using an artists air brush. The coupon was then submerged in 1M $CaCl_2$ for 45 to 60 min to complete cross-linking of the biopolymer gel. The estimated thickness of the coating was 40 μm. Finally, the tape was removed and the coupon placed in artificial sea water for 8 h.

*Scanning procedure*—The procedure for scanning was the same for both the control coupon and for the alginate coated coupon. The vessel holding the corroded coupon and the pH microelectrode (tip diameter = 50 μm) was positioned on the 3-D table for the scan. The electrode, as viewed through a binocular microscope, was moved to within approximately 50 μm of the metal surface using the 3-D positioner and held at that height (stationary z-axis) for the entire scan. There was no visible agitation of the solution in the reactor during scanning. The pH microelectrode was referenced to a silver/silver chloride electrode. The potential proportional to pH was measured with a Keithley Model 617 programmable electrometer that has an analog output proportional to the input from the electrode. This output was connected to a Keithley/Metrabyte model DAS-8 data acquisition board mounted in a Zenith 486DX PC. A map consisted of a matrix of data points, 40 rows by 40 columns, scanned one row at a time. Each row was scanned from the same direction to eliminate hysteresis in mechanical positioning. The mapped region covered the entire exposed portions of the coupons.

## Results and Discussion

Each coupon exhibited visually distinct regions after 8 h exposure to seawater. The control coupon displayed a reddish-orange deposit over its entire 0.04 $cm^2$ exposed surface, indicating significant corrosion. The coated region of the alginate-coated coupon also displayed a reddish-orange deposit indicative of corrosion, while the region outside of the coating appeared uncorroded.

Figure 4 shows a map of experimental pH data for the control coupon. The data is displayed in two formats; first, as a 3-D plot, and second, as a contour plot projected below the 3-D representation. The dip in pH matches the visible corrosion spot on the coupon. Figure 5 shows the map of experimental pH data for the calcium alginate coated coupon and is displayed in the same formats.

The entire exposed region of the control coupon displayed low pH values as well as visible corrosion. High pH was observed only at the edge of the exposed region.

Similar results were obtained for the calcium alginate coated surface. The reddish-orange cast, indicative of corrosion, rapidly developed in association with the alginate-coated zone; pH was lower above the same region. These observations were consistent with a rapidly corroding surface underneath the alginate, and a simultaneous transport of hydrogen ions through the alginate gel to the bulk water. Outside of the alginate coated zone, corrosion was less and the associated drop in pH was significantly lower.

The corrosion regions and associated pH differences were not unexpected on metal surfaces with both anodic and cathodic sites. The local interfacial equilibrium chemistry can be represented by Eqs 1 through 4.

$$Fe^0 \rightarrow Fe^{2+} + 2e^- \qquad \text{anodic region} \qquad (1)$$

$$Fe^{++} + 2H_2O \rightarrow Fe(OH)_2 + 2H^+ \qquad \text{hydrolysis} \qquad (2)$$

$$2Fe(OH)_2 + 1/2\ O_2 \rightarrow Fe_2O_3 + 2H_2O \qquad \text{further oxidation} \qquad (3)$$

$$2e^- + H_2O + 1/2\ O_2 \rightarrow 2OH^- \qquad \text{cathodic region} \qquad (4)$$

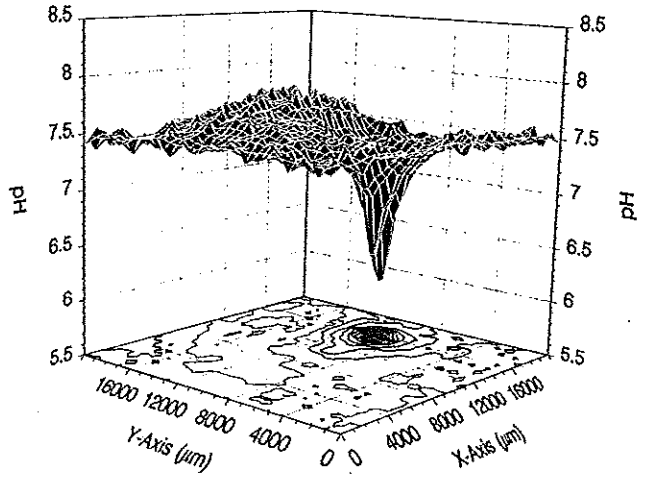


FIG. 4—*3D-map of pH at a fixed height (50 µm) above the surface of a freely-corroding mild steel coupon.*

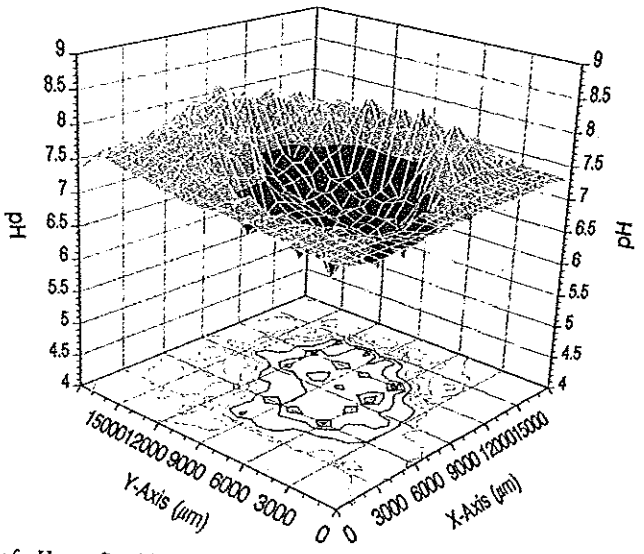


FIG. 5—*3D-map of pH at a fixed height (50 μM) above a calcium-alginate spot on a mild steel coupon.*

Comparing the two coupons revealed that corrosion in the uncoated region of the alginate-coated coupon was not as intense, nor did it develop as rapidly, as did corrosion on the control coupon. Both coupons were exposed to seawater for approximately the same length of time. In addition, pH above the control coupon was considerably lower than pH above the uncoated region of the alginate-coated coupon. It appears that the alginate coating stimulates formation of an anodic region beneath the coating that inhibits corrosion in the surrounding area. This preliminary observation is consistent with the concept that a patchy biofilm creates an electrochemical environment conducive to corrosion.

It is possible that the alginate coating on the coupon limits oxygen transport to the metal surface and, hence, creates a differential aeration cell [*16*]. In the bare area, this would encourage hydroxide ion generation and cathodic behavior, while in the alginate-coated region, anodic behavior and corrosion would result. This appears to be the case even though oxygen transport to metal below the alginate coating was expected to be nearly the same as that in the uncoated region, that is: (1) the system was stagnant and there was little or no convective mixing, (2) the alginate coating was thin, on the order of 100 μm; and (3) for small molecules, diffusion coefficients in calcium-alginate gels are nearly the same as in water [*17*]. LaQue [*18*] demonstrated that very small differences in oxygen mass transport, such as those created on rotating disks in aerated water, can produce differential aeration cells resulting in pronounced corrosion. Consequently, the very small oxygen gradients expected in our system could produce differential aeration cells similar to those seen by LaQue.

Another observation may suggest a second contributing factor. When the coupon is dried, the alginate coating can be peeled off the metal surface. And, when this is done, the red-orange ferric oxide remains with the alginate, exposing a bare, but somewhat dull, metal surface. It appears that the ferric oxide forms in the calcium-alginate gel rather than at the metal surface.

Alginic acid is a naturally occurring linear polymer consisting of manuronic and guluronic acid subunits. Each acid contains a carboxylic acid functional group. The affinity of calcium

alginate for divalent metal ions is well documented [*19–21*]. It is possible that in the presence of alginate gel, Eqs 2 and 3 can be expanded

$$\text{Alg-Ca} + \text{Fe}^{2+} \rightarrow \text{Alg-Fe} + \text{Ca}^{2+} \quad (5)$$

$$\text{Alg-Fe} + 1/4\ \text{O}_2 + \text{H}_2\text{O} \rightarrow 1/2\ \text{F}_2\text{O}_3 + 2\text{H}^+ + \text{Alg}^{2-} \quad (6)$$

$$\text{Alg}^{2-} + \text{Ca}^{2+} \rightarrow \text{Alg-Ca} \quad (7)$$

In Eqs 5 through 7, Alg is a binding site for a divalent metal ion in the alginate-gel polymer. It is possible that the Alg-complexed ferrous ion could oxidize more rapidly than the soluble hydrated ion, which is a catalytic effect. From mass action considerations, the decreased ferrous ion concentration could promote corrosion underneath the alginate coating.

These results may have significant implications for the mechanism of microbially influenced corrosion (MIC). If biopolymer alone can stimulate corrosion, then merely killing the microorganisms that form a biofilm will not stop MIC. In addition, if this is the principal mechanism for MIC, then there is little need to search for a mechanism involving viable organisms; instead, one should study the role of structural heterogeneity (patchiness) of biofilms in MIC.

## Conclusions

(1) The pH distribution above a corroding mild steel coupon was measured using an iridium oxide microelectrode in conjunction with a computer-controlled micropositioning system.

(2) Variations in pH were correlated with visible corrosion sites on the coupon. As expected, corrosion was associated with anodic regions of low pH adjacent to cathodic regions of high pH.

(3) Preliminary observations indicated that the presence of a calcium-alginate gel spot on the surface of mild steel influenced the corrosion process: (a) the mild steel surface under the gel spot corroded faster than the surrounding bare area and (b) the area surrounding the gel spot corroded more slowly than the surface of a bare-control coupon.

(4) Accelerated corrosion under the biopolymer gel could be due to either a differential aeration cell (crevice corrosion), or complexation of ferrous ion by the alginate gel, or some combination of the two processes.

## References

[*1*] Little, B. J., Wagner, P. A., Characklis, W. G., and Lee, W., *Biofilms*, W. G. Characklis and K. C. Marshall, Eds., John Wiley & Sons, New York, NY, 1990, pp. 635–670.

[*2*] Ford, T. and Mitchell, R., "The Ecology of Microbial Corrosion," *Advanced Microbial Ecology*, Vol. 17, 1990, pp. 231–262.

[*3*] Buchannan, R. A. and Stansburg, E. E., "Fundamentals of Coupled Electrochemical Reactions as Related to Microbially Influenced Corrosion," Proceedings, *Microbially Influenced Corrosion and Biodeterioration*, Knoxville, TN, Oct. 1990, N. J. Dowling, M. W. Mittleman, and J. C. Danko, Eds., University of Tennessee, Knoxville, 1990, pp. 1.11–1.17.

[*4*] Uhlig, H., *Corrosion and Corrosion Control*, John Wiley and Sons, New York, NY, 1971, p. 92.

[*5*] Bonnel, A., Dabosi, F., Deslouis, C., Duprat, M., Keddams, M., and Tribollet, B., "Corrosion Study of Carbon Steel in Neutral Chloride Solutions by Impedance Techniques," *Journal of the Electrochemical Social Society*, Vol. 130, 1983, p. 753.

[6] Hernandez-Deque, G., Pedersen, A., Thierry, D., Hermansson, M., and Kucera, V., "Bacterial Effects of Corrosion of Steel in Seawater," Proceedings, *Microbially Influenced Corrosion and Biodeterioration,* Knoxville, TN, Oct. 1990, N.J. Dowling, M. W. Mittleman, and J. C. Danko, Eds., University of Tennessee, Knoxville, 1990, pp. 2.41–2.51

[7] Smith, C. A., Compton, K. G., and Coley, F. H., "Aerobic Marine Bacteria and the Corrosion of Carbon Steel in Sea Water," *Corrosion Science,* Vol. 13, 1973, p. 677.

[8] Pope, D., Duquette, D., Wayner, P. C., Jr., and Arland, H. J., *Microbiologically Influenced Corrosion: A State-of-the-Art Review,* MTI Publication 13, Materials Technology Institute of the Chemical Process Industries, Inc., St. Louis, MO, June 1984.

[9] Iverson, W. P., "Microbial Corrosion of Iron," *Microbial Iron Metabolism,* J. B. Nieland, Ed., Academic Press, New York, NY, 1974, pp. 475–512.

[10] Costerton, J. W. and Boivin, J., "The Role of Biofilms in Microbial Corrosion," Proceedings, *Microbially Influenced Corrosion and Biodeterioration,* Knoxville, TN, Oct. 1990, N. J. Dowling, M. W. Mittleman, and J. C. Danko, Eds., University of Tennessee, Knoxville, 1990, pp. 5.85–5.89.

[11] VanHoudt, P., Lewandowski, Z., and Little, B., "Iridium Oxide pH Microelectrode," *Biotechnology and Bioengineering,* Vol. 40, 1992, pp. 601–608.

[12] Burke, L. D., Mulcahy, J. K., and Whelan, D. P., "Preparation of an Oxidized Iridium Electrode and the Variation of its Potential with pH," *Journal of Electroanalytical Chemistry,* Vol. 163, 1984, p. 117.

[13] Kinoshita, E., Ingman, F., Edwall, G., Thulin, S., and Glab, S., "Polycrystalline and Monocrystalline Antimony, Iridium and Palladium as Electrode Material for pH-Sensing Electrodes," *Talanta,* Vol. 33, 1986, pp. 125–134.

[14] Hitchman, M. L. and Ramanathan, S., "Evaluation of Iridium Oxide Electrodes Formed by Potential Cycling as pH Probes," *Analyst,* Vol. 113, 1988, pp. 35–39.

[15] Midgley, D., "A Review of pH Measurements at High Temperature," *Talanta,* Vol. 37, No. 8, 1990, pp. 767–781.

[16] Jones D., *Principles and Prevention of Corrosion,* MacMillan Publishing Company, New York, 1992, pp. 189–196.

[17] Tanaka, H., Matsumura, M., and Veliky, I. A., "Diffusion Characteristics of Substrates in Ca-Alginate Gel Beads," *Biotechnology and Bioengineering,* Vol. 26, 1984, pp. 53–58.

[18] Laque, F. L., "Theoretical Studies and Laboratory Techniques in Sea-Water Corrosion Testing Evaluation," *Corrosion,* Vol. 13, 1957, p. 303.

[19] Jang, L. K., Brand, W., Resong, M., Mainieri, W., and Geesey, G. G., "Feasibility of Using Alginate to Absorb Dissolved Copper from Aqueous Media," *Environmental Progress,* Vol. 9, 1990, pp. 269–274.

[20] Smidsrød, O. and Haug, A., "Dependence Upon Uronic Acid Composition of Some Ion-Exchange Properties of Alginates," *Acta Chemica Scandinavica,* Vol. 22, 1968, pp. 1989–1997.

[21] Smidsrød, O., "Molecular Basis for Some Physical Properties of Alginates in the Gel State," Faraday Discussions of the Chemical Society, Vol. 57, 1974, pp. 263–274.